Research article

Pablo Díaz-Núñez, Sabrina L. J. Thomä, Guillermo González-Rubio, Olivia Borrell-Grueiro, Roland P. M. Höller, Munish Chanana, David Garoz, Luis Bañares, Elena Junquera, Andrés Guerrero-Martínez*, Antonio Rivera* and Ovidio Peña-Rodríguez*

Rod–sphere cluster irradiation with femtosecond laser pulses: cut and paste at the nanoscale

https://doi.org/10.1515/nanoph-2021-0240
Received May 15, 2021; accepted August 3, 2021;
published online August 25, 2021

Abstract: We report on the irradiation of gold rod–sphere assemblies with ultrashort laser pulses, producing structures that are very difficult to obtain by other methods. The optical response of these assemblies displays several peaks arising from the interaction of the plasmon modes of the individual particles, offering thus great flexibility to control the energy deposited on the individual particles. Judicious selection of the wavelength and fluence of the laser pulses allow fine control over the changes produced: the particles can be melted, welded and/or the organic links cleaved. In this way, it is possible to generate structures "à la carte" with a degree of control unmatched by other synthetic protocols. The method is exemplified with gold nanoparticles, but it can be easily implemented on particles composed of different metals, widening considerably the range of possibilities. The final structures are excellent candidates for surface-enhanced spectroscopies or plasmonic photothermal therapy as they have a very intense electric field located outside the structure, not in the gaps.

Keywords: laser irradiation; nanoparticle welding; plasmonic assemblies.

***Corresponding authors: Andrés Guerrero-Martínez**, Departamento de Química Física, Universidad Complutense de Madrid, Avenida Complutense s/n, 28040, Madrid, Spain; and **Antonio Rivera and Ovidio Peña-Rodríguez**, Instituto de Fusión Nuclear "Guillermo Velarde", Universidad Politécnica de Madrid, José Gutiérrez Abascal 2, E-28006, Madrid, Spain; and Departamento de Ingeniería Energética, ETSII Industriales, Universidad Politécnica de Madrid, José Gutiérrez Abascal 2, E-28006, Madrid, Spain, E-mail: aguerrero@quim.ucm.es (A. Guerrero-Martínez), antonio.rivera@upm.es (A. Rivera), ovidio.pena@upm.es (O. Peña-Rodríguez). https://orcid.org/0000-0001-8576-2896 (A. Guerrero-artínez)
Pablo Díaz-Núñez, Instituto de Fusión Nuclear "Guillermo Velarde", Universidad Politécnica de Madrid, José Gutiérrez Abascal 2, E-28006, Madrid, Spain
Sabrina L. J. Thomä, Department of Chemistry II, University of Bayreuth, Universitätsstraße 30, D-95440 Bayreuth, Germany
Guillermo González-Rubio and Elena Junquera, Departamento de Química Física, Universidad Complutense de Madrid, Avenida Complutense s/n, 28040, Madrid, Spain
Olivia Borrell-Grueiro, Departamento de Química Física, Universidad Complutense de Madrid, Avenida Complutense s/n, 28040, Madrid, Spain; and INSTEC, Universidad de la Habana, Avenida Salvador Allende 1110, 6163, 10400, Habana, Cuba
Roland P. M. Höller, Department of Chemistry II, University of Bayreuth, Universitätsstraße 30, D-95440 Bayreuth, Germany; and Leibniz-Institut für Polymerforschung Dresden e.V., Institute of Physical Chemistry and Polymer Physics, Hohe Str. 6, 01069 Dresden, Germany. https://orcid.org/0000-0002-7329-0550
Munish Chanana, Department of Chemistry II, University of Bayreuth, Universitätsstraße 30, D-95440 Bayreuth, Germany; and Swiss Wood Solutions AG, Überlandstr. 129, CH-8600, Dübendorf, Switzerland
David Garoz, IMDEA Materials – Madrid Institute for Advanced Studies of Materials, c/Eric Kandel, 2, Parque Científico y Tecnológico| Tecnogetafe, 28906, Getafe, Madrid, Spain
Luis Bañares, Departamento de Química Física, Universidad Complutense de Madrid, Avenida Complutense s/n, 28040, Madrid, Spain; and Instituto Madrileño de Estudios Avanzados en Nanociencia (IMDEA Nanoscience), Cantoblanco, 28049, Madrid, Spain

1 Introduction

Electromagnetic waves can excite the free electrons of metal nanoparticles, inducing a phenomenon known as localized surface plasmon resonance (LSPR) [1–4]. Such LSPR can concentrate a huge amount of electromagnetic energy in nanometric volumes, offering the maximum possible spatial and temporal control over light [5–9]. LSPRs decay by re-emitting a photon, by creating very energetic electrons and holes (hot carriers), or by electron–phonon coupling [10–12]. The latter can produce very high local heating, up to thousands of Kelvin [13–15]. This heat is detrimental for most plasmonic devices, but recent studies indicate that it could be used to promote chemical reactions [16–18] or modify structures at the nanoscale [19–21].

The use of plasmonic nanostructures, combined with photocatalytic semiconductors, to favour chemical reactions by increasing the speed of interband transitions or

to extend the capture of light to photons below the bandgap has been, and remains, a very active area of research [22, 23]. Plasmonic or high-index dielectric nanostructures have been proposed to design ultra-thin semiconductor layers that, through the effects of field enhancement or light entrapment, achieve almost unitary broadband absorption with the consequent reduction in materials and device costs [24]. In contrast to semiconductor photocatalysis, transformations driven by hot carriers on metal surfaces offer the opportunity to explore new types of chemistry that are usually only possible at high temperatures and pressures [22].

On the other hand, the manufacture of complex nanoparticles constitutes a bottleneck for several applications because versatile preparation methods are typically very expensive and have a low yield, whereas the techniques that solve these problems do so by sacrificing versatility [25–27]. Despite being in its infancy, plasmon-assisted modification of structures at the nanoscale using ultra-short laser pulses has shown great potential to manufacture advanced nanostructures in a straightforward and efficient manner [19–21]. However, it has received comparatively much less attention than the production of plasmon-assisted chemical reactions.

The process can be understood as the union of different Lego pieces to produce complex nanostructures that are very difficult (or even impossible) to obtain by other means. The particles can be linked together with organic molecules, which is a well-established process [20, 28]. In turn, depending on the fluence, laser pulses can deposit sufficient energy on the particles to melt them or produce a temperature increase that, although not enough to melt the particles, may degrade the organic ligand that links them together. In this way, it is possible to selectively cleave organic bonds or weld neighbouring particles together [19, 20]. Assemblies involving asymmetric particles offer extra flexibility because they have different plasmonic modes. Hence, we can easily devise the irradiation conditions (i.e., laser wavelength and fluence) to weld some particles together and unlink others.

In this work, we have taken advantage of this versatility to illustrate a process to fabricate unique structures beyond the possibilities offered by current manufacturing methods. This two-step process is schematically depicted in Figure 1. First, we synthesized rod–sphere core–satellite nanoclusters using bovine serum albumin as the linker (Figure 1(a)) [28], which are then irradiated with femtosecond (fs) laser pulses (Figure 1(b)). Depending on the energy deposited, the spheres were found to weld onto the rod or the organic links cleaved, releasing the spheres from the structure.

2 Results and discussion

Spherical Au nanoparticles with an approximate diameter of 15.5 ± 3 nm were synthesized via the Turkevich reduction method [29]. Likewise, Au nanorods were synthesized using a process that we have described elsewhere [20, 21, 30], with a length of 63 ± 7 nm, a diameter of 20 ± 4 nm and an aspect ratio of 3.2 ± 0.7. Figure 2(a) shows the UV–Vis spectra of the nanorod (continuous lines) and nanocluster (dashed lines) dispersions, prior to any irradiation. The aggregation of satellite particles produces a redshift of the LSPR band, accompanied by widening and a significant intensity drop. This LSPR displacement can be explained by the complex interaction between the plasmon modes of the different structures that make up the cluster. On the other hand, the observed plasmon widening and weakening is the result of a large number of possible combinations to form assemblies, each with an LSPR maximum located at a slightly different wavelength.

Rod–sphere assemblies have the LSPR maximum located at 791 nm, nearly matching the wavelength of the laser pulses (800 nm). A summary of the changes produced upon irradiation on the optical response of the rod–sphere clusters is depicted in Figure 2(b). No significant changes were observed in the case of irradiation at 0.5 J/m^2 for 12 min (not shown). From a fluence of 1 J/m^2 upwards, a drop in absorption was observed at 800 nm, which became more pronounced with the increasing fluence. At the same time, an enhancement of the optical density was observed on the right side of the LSPR, at wavelengths above that of the laser pulse. In this way, the single plasmon mode observed in the original clusters splits in two upon irradiation, increasing the separation between the two peaks with the fluence. For the lowest fluences, we carried out additional irradiations for 1 h, observing, at 0.5 J/m^2, a change similar to that occurring at higher fluences and, at

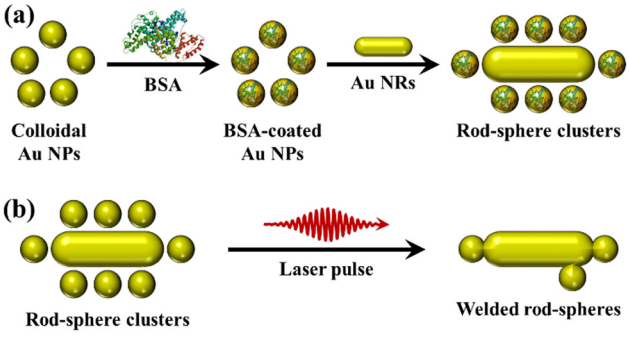

Figure 1: Schematic representation of (a) synthesis of Au rod–sphere nanoclusters and (b) welding of those nanoclusters by irradiation with fs laser pulses.

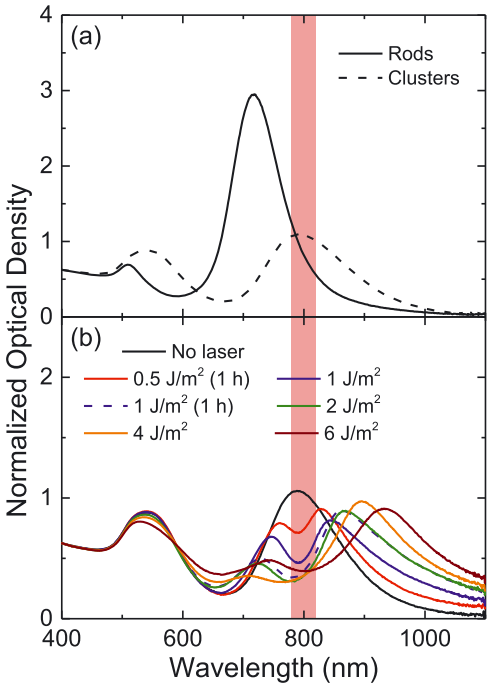

Figure 2: Experimental UV–Vis spectra of (a) bare rods (continuous lines) and rod–sphere clusters (dashed lines) and (b) rod–sphere clusters, before and after irradiation at the fluences indicated in the graph. Unless indicated otherwise, irradiation was performed for 12 min. The red vertical band represents the spectral extent of the 50 fs laser pulses.

1 J/m^2, the peak splitting becoming much more pronounced, to the extent that the spectrum obtained for these conditions was similar to that obtained at 2 J/m^2 and 12 min.

Figure 3 shows typical transmission electron microscope (TEM) images of both, non-irradiated and irradiated structures, at the different fluences used. No significant differences are observed between the non-irradiated particles (Figure 3(a) and (b)) and those irradiated at 0.5 J/m^2 (Figure 3(c)), indicating that the number of structures modified at this fluence is very low. With the increasing fluence, for example, at 1 and 2 J/m^2 (Figure 3(d) and (e), respectively), we observe new structures appear with spheres welded to the rod tips, while the side particles seem to remain unaffected. The number of structures presenting spheres welded to the rod tips increased with the fluence. At a fluence of 4 J/m^2 (Figure 3(f)), most spheres at the tips have been welded to the core rod, while the side spheres have disappeared, indicating that in all likelihood some material has molten at the tips whereas the rod and/or side spheres have reached a temperature high enough to break the organic bonds linking them. Finally, at 6 J/m^2 (Figure 3(g)), it is observed that all the spheres have been welded to the central rod and even some spheres have been welded together, a clear sign of partial gold melting. However, it is noticeable that in all cases the rods conserve their shape, which means that they have not molten (except at the tips), or they would have a spherical shape [21, 30].

To better understand the experimental results, we performed finite-differences in the time-domain (FDTD) simulations of the optical response for some selected structures, using the free software computer code MIT electromagnetic equation propagation (MEEP) [31]. We began with non-irradiated structures, where the particles

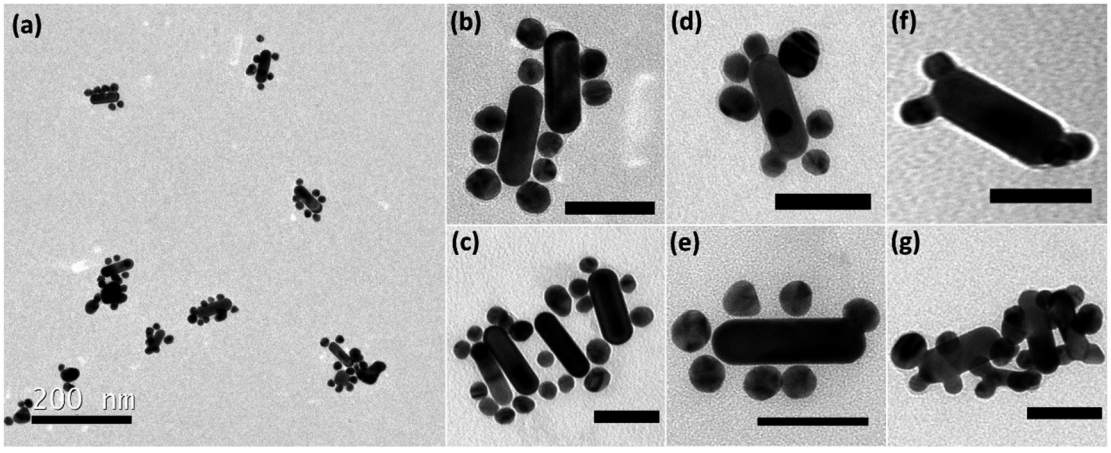

Figure 3: TEM micrographs of typical rod–sphere clusters obtained, (a) low and (b) high magnification images before irradiation and high magnification images after irradiation with laser pulses at a fluence of (c) 0.5, (d) 1.0, (e) 2.0, (f) 4.0 and (g) 6.0 J/m^2. The irradiation time in all cases is 12 min. The scale bars represent 200 nm in (a) and 50 nm in all other images.

are separated from each other (from TEM measurements we determined that the separation between the rod and the spheres is 3 nm), as shown in Figure 4. When two spheres are added at the tips of the rod, the plasmon is redshifted with respect to the spectrum of the original rod (not shown). As more spheres are added, the redshift increases and a new mode, much less intense, appears around 580 nm, possibly produced by the interaction between neighbouring spheres. The enhancement of the electric field around the structure (Figure 4(b)–(e)) shows no significant changes when more spheres are added to the system. The maximum value always appears at the gap between the rod and the spheres and, only in the case with eight spheres, also in the gap between the side spheres. From the point of view of irradiation, a very important aspect of the shift of the LSPR maximum is that laser pulses will affect preferentially certain structures (those with the LSPR in resonance with the laser wavelength). In this particular case, 800 nm pulses will have a greater effect on structures with fewer spheres, although the ones with more spheres will also receive significant amounts of energy. One important aspect to interpret the results shown in Figure 4 is that the clusters studied in this work are formed around a nanorod. Consequently, their optical response (and the amount of energy that they absorb) depends strongly on their orientation with respect to the polarization of the laser pulse [20, 21]. Therefore, the efficiencies shown in Figure 4 should only be interpreted as the upper limit. The random movement of the structures within a colloid means that, for most pulses, the structure will not be perfectly aligned with the laser polarization and, consequently, they will receive much less energy than that estimated for perfect alignment.

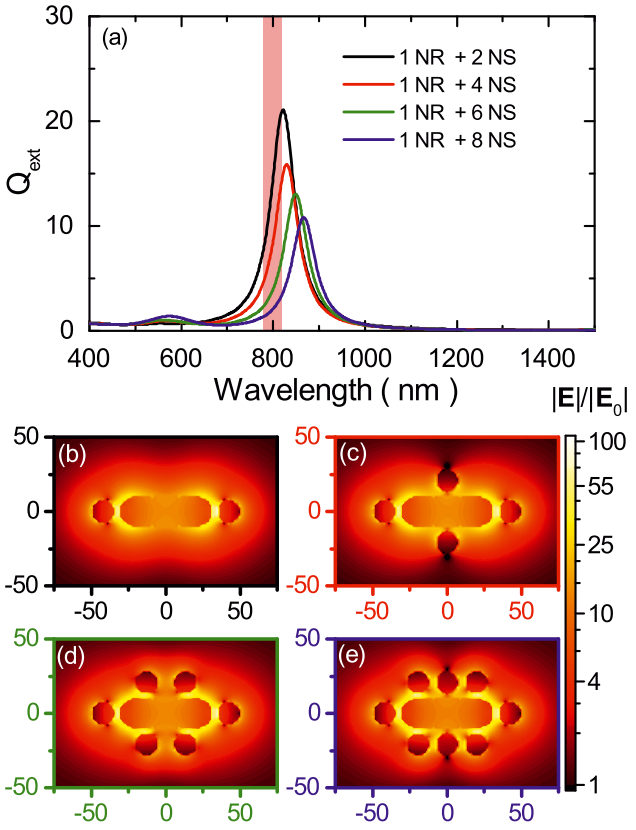

Figure 4: (a) Simulated extinction efficiency (Q_{ext}) calculated for different structures, composed of a nanorod surrounded by a varying number of satellite spheres, as indicated in the legend. Electric field enhancement, calculated for the wavelength of the LSPR maximum, in the surroundings of the following structures: (b) one rod with two spheres at the tips, (c) one rod with two spheres at the tips and two at the sides, (d) one rod with two spheres at the tips and four at the sides, (e) one rod with two spheres at the tips and six at the sides. The separation between the rod and the spheres is 3 nm. In all cases, the light polarization is along the rod axis and the wave vector is coming out of the plane. The red vertical band represents the spectral extent of the 50 fs laser pulses.

Figure 5 shows the simulated optical response of the welded structures. The main effect of welding is a significant redshift of the plasmon band, which can be explained by assuming that the structure with the spheres at the tip behaves like a single rod with a larger aspect ratio. On the other hand, the split of the plasmon peak (also observed in the experimental spectra) can be explained by two different plasmonic modes that arise in the new structure, as can be seen in Figure S4. The peak located at the lower wavelength comes mainly from the interaction of the rod and the spheres at the tips (Figure S4(b)) whereas the high-wavelength peak is related to the interaction of the rod with all of the spheres, and also between the side spheres (Figure S4(c)). It should be noted that the modified structures barely absorb the laser pulses. In practice, this means that, once the structures have been welded, they do not suffer any further evolution. For this reason, the changes observed in the optical spectrum as a function of the irradiation time should be interpreted as the modification of structures previously unaffected by the laser pulses. In other words, the modification of the structure is a single-pulse process but the irradiation time plays an important role in the final results because (i) with high probability, several pulses are necessary until the structure absorbs enough energy and (ii) it cannot be discarded that a certain cumulative effect exists, where one pulse modifies slightly the structure and then another pulse deposits enough energy to produce important changes. One important feature of the electric near fields of the welded structures is that the maximum enhancement is obtained outside the structure

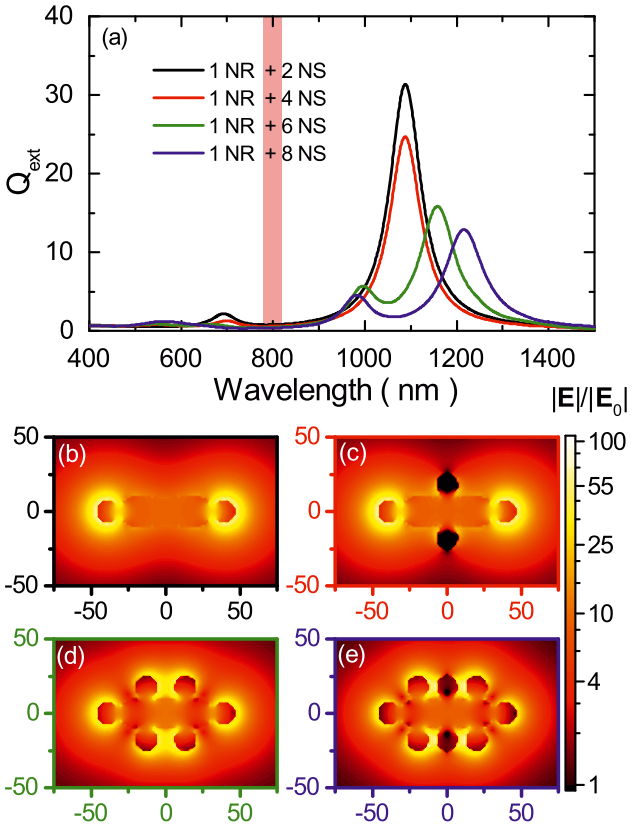

Figure 5: (a) Simulated extinction efficiency (Q_{ext}) calculated for different structures, composed of a nanorod surrounded by a varying number of satellite spheres, as indicated in the legend. Electric field enhancement, calculated for the wavelength of the LSPR maximum, in the surroundings of the following structures: (b) one rod with two spheres at the tips, (c) one rod with two spheres at the tips and two at the sides, (d) one rod with two spheres at the tips and four at the sides, (e) one rod with two spheres at the tips and six at the sides. The rod and the spheres are touching each other and a small cylinder, with a diameter of 10 nm, was added to connect them, mimicking the morphology of the welded volume observed experimentally. In all cases, the light polarization is along the rod axis and the wave vector is coming out of the plane. The red vertical band represents the spectral extent of the 50 fs laser pulses.

(*i.e.*, not in the gaps), which would facilitate the access of molecules in surface-enhanced spectroscopies.

The key to understanding the described results lies in knowing how much energy is absorbed by each of the particles in the structure and how they evolve after rapidly reaching the maximum temperature (in a process that is practically adiabatic), *i.e.*, during the cooling down [32]. A detailed calculation is very complicated; hence, we will simplify it here only for a structure consisting of a rod with a sphere at each tip, as shown in Figure 6. However, this does not weaken the generality of the conclusions, because the experimental results (Figure 3) show that, for the conditions of this work, most modifications occur in the spheres located at the rod tips. This can also be understood from the FDTD simulations (see Figure 4) because the wavelength of the laser pulses excites only the longitudinal mode of the structures. The effective absorption cross-section of each of the three particles is shown in Figure 6(a). Using these values, it can be determined that the rod absorbs approximately 97% of the energy at the laser wavelength (800 nm) and each sphere only 1.5% (see figure inset).

Taking into account the relative amount of energy absorbed by each particle and the specific heat capacity of gold [33, 34], one can estimate the maximum temperature that they reach during adiabatic heating. For instance, at a fluence of 4 J/m^2, the rod reaches a temperature of 1915 K, while that of the spheres is 700 K, approximately. Under these conditions, the rod is expected to melt and, subsequently, evolve to a sphere (the most stable shape) [21, 30]. However, this is not observed experimentally, suggesting that there must be an additional mechanism suppressing the evolution from rod to sphere. To better understand this effect, we performed finite elements method (FEM) calculations to study the temperature kinetics of this rod–sphere system (Figure 6(b)). Two cases were considered: (i) the rod

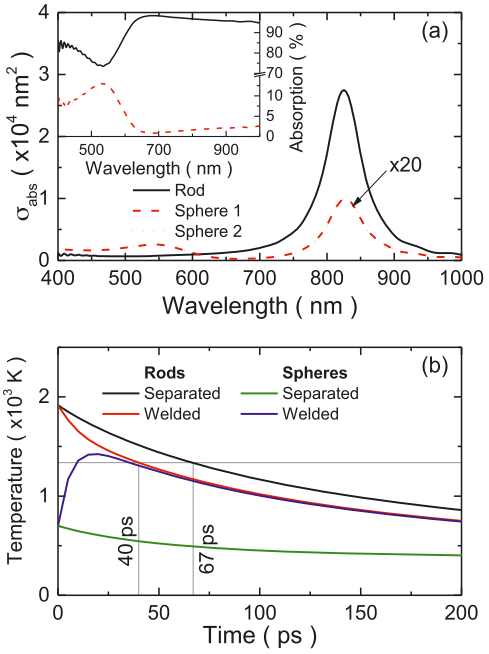

Figure 6: (a) Absorption cross-section (σ_{abs}) of the individual particles forming the structure of a rod with two spheres at the tips. The inset represents the relative absorption for each particle: the rod absorbs over 95% of the energy. (b) Temperature evolution of the rod and the spheres when they are separated 2 nm (black and green lines, respectively) or welded (red and blue lines). The grey horizontal line represents the melting temperature of bulk gold. The grey vertical lines represent the time when the rod temperature falls below the melting point of bulk gold.

and the spheres remain separated (2 nm) after heating and (ii) they come into contact (for instance, due to rod expansion). In both cases, the particles have been assumed to be immersed in water, similar to the case reported by Ekici et al. [33]. In Figure 6(b), we can see that, when the particles remain separated, the rod reaches the melting temperature of gold and remains above it for 67 ps (and probably much longer in realistic conditions, due to the reduced dissipation produced by the coating protein, which acts as a thermal barrier). Under these conditions, and depending on the cooling time, the rod could evolve into a sphere. On the other hand, when the rod is in contact with the spheres, their temperatures equilibrate in a very short time and the rod temperature falls below the melting point in just 40 ps, regardless of the protein coverage (this effect could be more pronounced in realistic cases with more than two spheres). This explains why the rod structure is preserved, even at the highest fluence (6 J/m^2) while, at fluences of 2 J/m^2 and beyond, we see welded spheres, indicating that, in all likelihood, they have come into contact at high temperature. Finally, it is interesting to compare the results at fluences of 4 and 6 J/m^2. For the former case, the side spheres are absent, whereas for the latter fluence the spheres are welded. Tentatively, we can ascribe the difference to the temperatures reached by the side spheres. Particles weld when they get in contact at a high enough temperature. Initially, the energy absorbed by side spheres is very low compared to that absorbed by spheres at the tips. Thus, only irradiations at very high fluence lead to temperatures compatible with welding. At 4 J/m^2, the temperature raise apparently only produces link breakage and as a result the release of the side spheres, but not permanent welding.

3 Conclusions

In summary, we report here the irradiation of gold rod–sphere assemblies with ultrashort laser pulses, allowing us to manufacture structures that are very difficult to obtain by other methods. The proposed methodology is a two-step process. First, a protein-assisted assembly is employed to fabricate nanoclusters with a large number of satellite particles per rod. The rod–sphere assemblies exhibit two plasmon modes, redshifted with respect to the transversal and longitudinal modes of the core rod. By varying the aspect ratio of the core particle, these plasmon bands can be tuned so that a nanocluster with the LSPR located around 800 nm can be obtained (791 nm). Next, the assemblies are irradiated with a near-infrared fs laser (wavelength 800 nm; 50 fs; 0.5–6 J/m^2). The optical properties of the nanocluster dispersions are notably modified upon irradiation: the plasmon band located at the highest wavelength splits, being more pronounced the effect with the increasing laser fluence. TEM analysis revealed that, starting at a fluence of 1 J/m^2 for 1 h, some spheres weld to the tips of the rods. More particles become welded as the fluence increases. At 4 J/m^2, the tip spheres are welded whereas the side spheres are removed and, finally, both, the tip and side spheres, weld to the rod and between themselves at a fluence of 6 J/m^2.

FDTD and FEM simulations have allowed us to understand these results in terms of how much energy is absorbed by each particle and how the temperature of the system evolves during heating. The proposed approach offers great flexibility from the viewpoint of control over the changes produced on the irradiated assemblies. Judicious selection of the wavelength and fluence of the laser pulses would allow fine control over the changes induced. In this way, it is possible to generate custom-made structures with a degree of control that is hard to match by other synthetic methods. The method has been exemplified for gold nanoparticles, but it should be easy to implement for particles composed of different metals, expanding considerably the range of possibilities of this methodology. For example, we can envisage assemblies composed of gold and platinum particles, so that the resulting bimetallic structure has an intense plasmon combined with catalytic properties. Finally, the structures manufactured by this method exhibit a very intense enhancement of the electric field outside the structure (not just in the gaps). Hence, these structures are excellent candidates for surface-enhanced spectroscopies or plasmonic photothermal therapy.

Acknowledgements: Femtosecond laser resources provided by the Center for Ultrafast Lasers of Complutense University of Madrid are gratefully acknowledged. The authors acknowledge the computer resources and technical assistance provided by the Centro de Supercomputación y Visualización de Madrid (CeSViMa) and the supercomputing infrastructure of the NLHPC (ECM-02). This paper is based upon work from COST Action TUMIEE (CA17126).

Author contributions: All the authors have accepted responsibility for the entire content of this submitted manuscript and approved submission.

Research funding: This work has been funded by the Spanish Ministry of Science, Innovation and Universities (MICIU) (grants RTI2018-095844-B-I00, PGC2018-096444-B-I00, PID2019-105325RB-C32 and MAT2017-86659-R), the EUROfusion Consortium through project ENR-IFE19.CCFE-01 and the Madrid Regional Government (grants P2018/NMT-4389 and P2018/EMT-4437).

Conflict of interest statement: The authors declare no conflicts of interest regarding this article.

References

[1] S. A. Maier, *Plasmonics: Fundamentals and Applications*, 1st ed. New York, Springer, 2007.

[2] J. Heber, "Plasmonics: surfing the wave," *Nature*, vol. 461, pp. 720–722, 2009.

[3] S. Lee, A. Reuveny, J. Reeder, et al., "Where now for plasmonics?" *Nat. Nanotechnol.*, vol. 11, p. 1, 2016.

[4] M. L. Brongersma and V. M. Shalaev, "The case for plasmonics," *Science*, vol. 328, pp. 440–441, 2010.

[5] J. A. Schuller, E. S. Barnard, W. Cai, Y. C. Jun, J. S. White, and M. L. Brongersma, "Plasmonics for extreme light concentration and manipulation," *Nat. Mater.*, vol. 9, pp. 193–204, 2010.

[6] T. Qiu, Y. Zhou, J. Li, et al., "Hot spots in highly Raman-enhancing silver nano-dendrites," *J. Phys. Appl. Phys.*, vol. 42, p. 175403, 2009.

[7] G. Baffou, C. Girard, and R. Quidant, "Mapping heat origin in plasmonic structures," *Phys. Rev. Lett.*, vol. 104, p. 136805, 2010.

[8] H. Wei and H. Xu, "Hot spots in different metal nanostructures for plasmon-enhanced Raman spectroscopy," *Nanoscale*, vol. 5, pp. 10794–10805, 2013.

[9] P. Díaz-Núñez, J. M. García-Martín, M. U. González, et al., "On the large near-field enhancement on nanocolumnar gold substrates," *Sci. Rep.*, vol. 9, p. 13933, 2019.

[10] G. V. Hartland, L. V. Besteiro, P. Johns, and A. O. Govorov, "What's so hot about electrons in metal nanoparticles?" *ACS Energy Lett.*, vol. 2, pp. 1641–1653, 2017.

[11] T. G. White, P. Mabey, D. O. Gericke, et al., "Electron-phonon equilibration in laser-heated gold films," *Phys. Rev. B*, vol. 90, p. 014305, 2014.

[12] J. Grossi, J. Kohanoff, T. N. Todorov, E. Artacho, and E. M. Bringa, "Electronic heat transport versus atomic heating in irradiated short metallic nanowires," *Phys. Rev. B*, vol. 100, p. 155434, 2019.

[13] G. Baffou, M. P. Kreuzer, F. Kulzer, and R. Quidant, "Temperature mapping near plasmonic nanostructures using fluorescence polarization anisotropy," *Opt. Express*, vol. 17, p. 3291, 2009.

[14] G. Baffou, R. Quidant, and C. Girard, "Heat generation in plasmonic nanostructures: influence of morphology," *Appl. Phys. Lett.*, vol. 94, p. 153109, 2009.

[15] G. Baffou and R. Quidant, "Thermo-plasmonics: using metallic nanostructures as nano-sources of heat," *Laser Photonics Rev.*, vol. 7, pp. 171–187, 2013.

[16] M. Kim, M. Lin, J. Son, H. Xu, and J.-M. Nam, "Hot-electron-mediated photochemical reactions: principles, recent advances, and challenges," *Adv. Opt. Mater.*, vol. 5, p. 1700004, 2017.

[17] W. Ni, H. Ba, A. A. Lutich, F. Jäckel, and J. Feldmann, "Enhancing single-nanoparticle surface-chemistry by plasmonic overheating in an optical trap," *Nano Lett.*, vol. 12, pp. 4647–4650, 2012.

[18] H. Zhu, H. Xie, Y. Yang, et al., "Mapping hot electron response of individual gold nanocrystals on a TiO_2 photoanode," *Nano Lett.*, vol. 20, pp. 2423–2431, 2020.

[19] L. O. Herrmann, V. K. Valev, C. Tserkezis, et al., "Threading plasmonic nanoparticle strings with light," *Nat. Commun.*, vol. 5, p. 4568, 2014.

[20] G. González-Rubio, J. González-Izquierdo, L. Bañares, et al., "Femtosecond laser-controlled tip-to-tip assembly and welding of gold nanorods," *Nano Lett.*, vol. 15, pp. 8282–8288, 2015.

[21] G. González-Rubio, P. Díaz-Núñez, A. Rivera, et al., "Femtosecond laser reshaping yields gold nanorods with ultranarrow surface plasmon resonances," *Science*, vol. 358, pp. 640–644, 2017.

[22] M. L. Brongersma, N. J. Halas, and P. Nordlander, "Plasmon-induced hot carrier science and technology," *Nat. Nanotechnol.*, vol. 10, pp. 25–34, 2015.

[23] A. Naldoni, U. Guler, Z. Wang, et al., "Broadband hot-electron collection for solar water splitting with plasmonic titanium nitride," *Adv. Opt. Mater.*, vol. 5, p. 1601031, 2017.

[24] A. Naldoni, V. M. Shalaev, and M. L. Brongersma, "Applying plasmonics to a sustainable future," *Science*, vol. 356, pp. 908–909, 2017.

[25] X. Zhang, C. Sun, and N. Fang, "Manufacturing at nanoscale: top-down, bottom-up and system engineering," *J. Nanoparticle Res.*, vol. 6, pp. 125–130, 2004.

[26] B. Frank, X. Yin, M. Schäferling, et al., "Large-area 3D chiral plasmonic structures," *ACS Nano*, vol. 7, pp. 6321–6329, 2013.

[27] P. Gao, X. Li, Z. Zhao, et al., "Pushing the plasmonic imaging nanolithography to nano-manufacturing," *Opt. Commun.*, vol. 404, pp. 62–72, 2017.

[28] R. P. M. Höller, M. Dulle, S. Thomä, et al., "Protein-assisted assembly of modular 3D plasmonic raspberry-like core/satellite nanoclusters: correlation of structure and optical properties," *ACS Nano*, vol. 10, pp. 5740–5750, 2016.

[29] J. Turkevich, P. C. Stevenson, and J. Hillier, "A study of the nucleation and growth processes in the synthesis of colloidal gold," *Discuss. Faraday Soc.*, vol. 11, pp. 55–75, 1951.

[30] P. Díaz-Nuñez, G. González-Rubio, A. Prada, et al., "Using femtosecond laser irradiation to grow the belly of gold nanorods," *J. Phys. Chem. C*, vol. 122, pp. 19816–19822, 2018.

[31] A. F. Oskooi, D. Roundy, M. Ibanescu, P. Bermel, J. D. Joannopoulos, and S. G. Johnson, "Meep: A flexible free-software package for electromagnetic simulations by the FDTD method," *Comput. Phys. Commun.*, vol. 181, pp. 687–702, 2010.

[32] J. C. Castro-Palacio, K. Ladutenko, A. Prada, et al., "Hollow gold nanoparticles produced by femtosecond laser irradiation," *J. Phys. Chem. Lett.*, vol. 11, pp. 5108–5114, 2020.

[33] O. Ekici, R. K. Harrison, N. J. Durr, D. S. Eversole, M. Lee, and A. Ben-Yakar, "Thermal analysis of gold nanorods heated with femtosecond laser pulses," *J. Phys. Appl. Phys.*, vol. 41, p. 185501, 2008.

[34] I. Barin, *Thermochemical Data of Pure Substances*, 3rd ed. Weinheim, Wiley, 1995.

Supplementary Material: The online version of this article offers supplementary material (https://doi.org/10.1515/nanoph-2021-0240).